The effect of impactor shape on low velocity impact behavior of cylindrical sandwich structures with trapeozidal core

Ilyas Bozkurt¹* iD

¹Department of Mechanical Engineering, Architecture and Engineering Faculty, Mus Alparslan University, 49250 Mus, Türkiye

Abstract: The aim of this study is to investigate the impact performance of a cylindrical sandwich structure with Trapeozidal core under different geometries of impactors using the finite element method. The effects of impactor shape, facesheets thickness and impact point on peak contact force, absorbed energy efficiency, maximum displacement and damage deformation are investigated. *Progressive damage analysis* based on the *Hashin damage criterion* was performed using *MAT 54* material model in *LS DYNA* finite element program for low velocity simulations. The impact behavior was investigated by creating a *Cohesive Zone Model (CZM)* based on *bilinear traction-separation law* while providing the connection between the core structure and its surfaces. At the end of the study, it was determined that the contact force values at P2 were higher than P1. Peak force variation values for cylinder, cone and sphere tipped impactors at P1 and P2 points were 43.5%, 132.3% and 62.2%, respectively. Core support has a significant effect on the contact force. The peak force value and energy absorption efficiency value obtained with the Cone impactor are higher than the others. For all three impactors, it was determined that the largest and dominant damage type was matrix damage.

Keywords: impactor shape; cylindrical sandwich composite; Impact test; Progressive damage analysis; Finite element method; cohesive zone model (CZM).

1. Introduction

Composite structures are effectively used in many sectors, especially in the aerospace industry, due to their high strength-to-weight ratio [1]. Especially with the recent technological developments and the development of production machines and production methods, composite structures have started to be used in many areas in our daily lives, from bicycle bodies to car steering wheels, from laptop cases to shoe fabrics. In addition, the rate of use of composite structures in airplanes and cars carrying life and property is increasing day by day. However, their performance decreases due to the loads they are exposed to in application areas and during service [2]. These structures used in different areas can be subjected to loads and impacts of very different types and magnitudes. Due to these loads, the service life of the damaged structure decreases. This can cause major disasters and huge cost losses during service. Therefore, researchers and engineers working in this field should determine the type of impact and the type of impactor that composite structures will be exposed to, and make appropriate material selection and structure selection by predicting the reaction of the structure to it.

Sandwich structures are structures formed by the combination of core and facesheet structures and are widely used in the field of engineering. These structures, which are usually produced flat, can be produced in many different shapes, curved or cylindrical, with the advancement of technological developments and production techniques. These structures are used in many areas of our lives, such as airplane tips or new generation lightweight bicycle bodies, without even realizing it.

In general, when metal materials are subjected to impact, the material behavior can be predicted due to the linearity in their structure. However, in composite structures, it is more difficult to make this prediction due to the complexity of the micro-mechanical structure of the material. Because in these structures, there are many factors affecting the material strength such as fiber type, matrix type, fiber and matrix ratio, fiber and matrix compatibility. All of these have an effect on material mechanics to some extent. Therefore, it is very difficult to predict all these possibilities in advance. For this reason, researchers conduct research on the mechanical performance of composite structures in laboratory environments or with the help of numerical analysis.

Many specialized machines and devices have been developed for the manufacturing of composite structures and the determination of their mechanical properties. Many special devices must be used for the mechanical properties of composite structures produced using high-cost consumables. In institutions where laboratory facilities are limited and financial support is limited, researchers cannot carry out healthy studies in this field. To overcome this problem, researchers have been able to investigate the mechanical behavior of composite structures with the finite element method. In addition, even some complex and difficult experiments can be applied with high accuracy precision with the finite element method.

There are many studies investigating the behavior of sandwich composite structures with high impact absorption potential under impact [2-12]. Li et al. [13] experimentally and numerically investigated the effects of impactor in corrugated sandwich structures with carbon fiber reinforced polymer (CFRP) facesheets and aluminum cores. Low-velocity impact tests were carried out to study the impact resistance when impacted by conical, hemispherical and flat impactors. They applied a progressive damage model based on Hashin fracture criteria and Yeh delamination fracture criteria in *ABAQUS/ Explicit*. Khalkhali et al. [14] investigated the nonlinear low-velocity impact response of a sandwich plate subjected to impacts with different geometric shapes. The sandwich plate is assumed to consist of two face layers reinforced with CNTs graded as X profile along their thickness and a homogeneous core. They experimentally carried out impact tests using three different impactors: spherical impactor, conical impactor, and cylindrical impactor. Shirbhate et al. [15] examined the explosion response of a hexagonal honeycomb sandwich structure with holes along the cell height of the core compared to conventional honeycomb cores. Yalkın et al. [16] numerically investigated the low-velocity impact properties of E-glass fiber/epoxy and PVC foam core sandwich composite configurations. Damghani et al. [17] simulated the impact behavior of aluminum foam core sandwich structures with *LS-DYNA* software.

In this study, unlike the literature, the impact perfor-

mance of cylindrical sandwich CFRP composite structure with Trapeozidal core was investigated by the finite element method. The effects of impactor shape and facesheets thickness on peak contact force, absorbed energy efficiency, maximum displacement and damage deformation were investigated. Progressive damage analysis based on the Progressive damage analysis based on the *Hashin damage criterion* was performed using *MAT 54* material model in *LS DYNA* finite element program for low velocity simulations.

2. Materials and Methods

2.1. Finite Element Model

The dimensional details of the cylindrical sandwich structure with Trapeozidal core are given in ▶**Figure 1**. Impact tests will be applied to the sandwich structure with different geometry impactors. The specimens, which were drawn as a flat plate, were twisted with the Flex command in Solidworks and brought to a cylindrical shape. In this structure with diameter x length dimensions of 100 x 140 mm, impact performances were also examined by using two different facesheets with thicknesses of 2 mm and 4 mm. Low velocity impact simulation was modeled as shown in ▶**Figure 2**. All impact tests were applied to the center of the specimens. The top and bottom holders were fixed. The impactor was limited to displacements in the x and y directions and could only move in the direction of the impactor (z-axis). Although the run time of the analysis with the shell element was fast, an eight-node solid element (*ELFORM1*) was used to show the damage structures more clearly and realistically.

This element structure is given in ▶**Figure 3** for the impactors used in the study. A mesh element size of 2x2 mm was chosen by mesh convergence and considering the processing time. In total, 30197 nodes and 26750 solid elements were used. The CONTACT ERODING SURFACE TO SURFACE contact card was used to define the contact between the impactor and the cylindrical sandwich structure. The CONTACT AUTOMATIC SURFACE TO SURFACE contact card was used to ensure that the specimen between the grippers does not move during impact and is held stationary by the gripper. The static and dynamic friction coefficients were entered as 0.2 and 0.3 respectively [18].

Since the core structure used in the study is corrugated, it does not contact everywhere in the specimen in the same way. Therefore, while there is core support at some points where the impactor is applied, there is core support in some places. Impact tests were performed at two different points in the study. Impact points are given in ▶**Figure 4**. The impact performances of these points were also compared.

2.2. Modeling of adhesive layer

Sandwich composite structures are composed of top and bottom surfaces and the core structure between them. To model the adhesive behavior between these two elements, the CZM model with a bilinear trac-

tion-separation law has been developed. This law is based on the application of 3 independent parameters. The traction t_0, between the layers when the force is applied, the separation distance δ_0 when the damage starts and G_C under this curve. After the impact occurs, the separation between the layers occurs according to this principle (▶Figure 5)
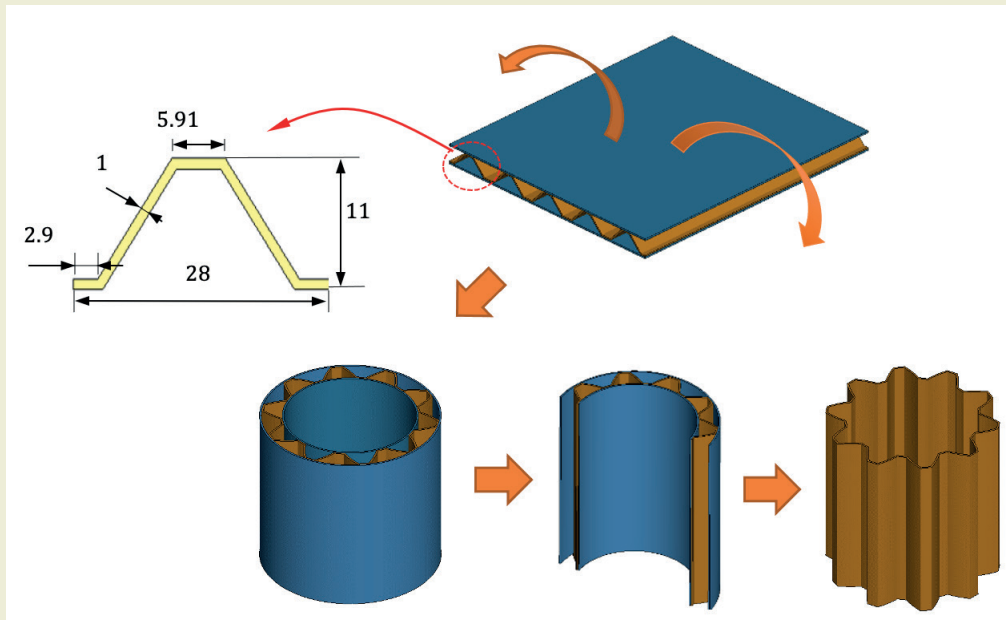
Figure 1. Specimen dimensions.

Solid element
(ELFORM1)

1-Upper composite face sheet
2-Trapeozidal core
3-Lower composite face sheet
4-Impactor
5-Holder
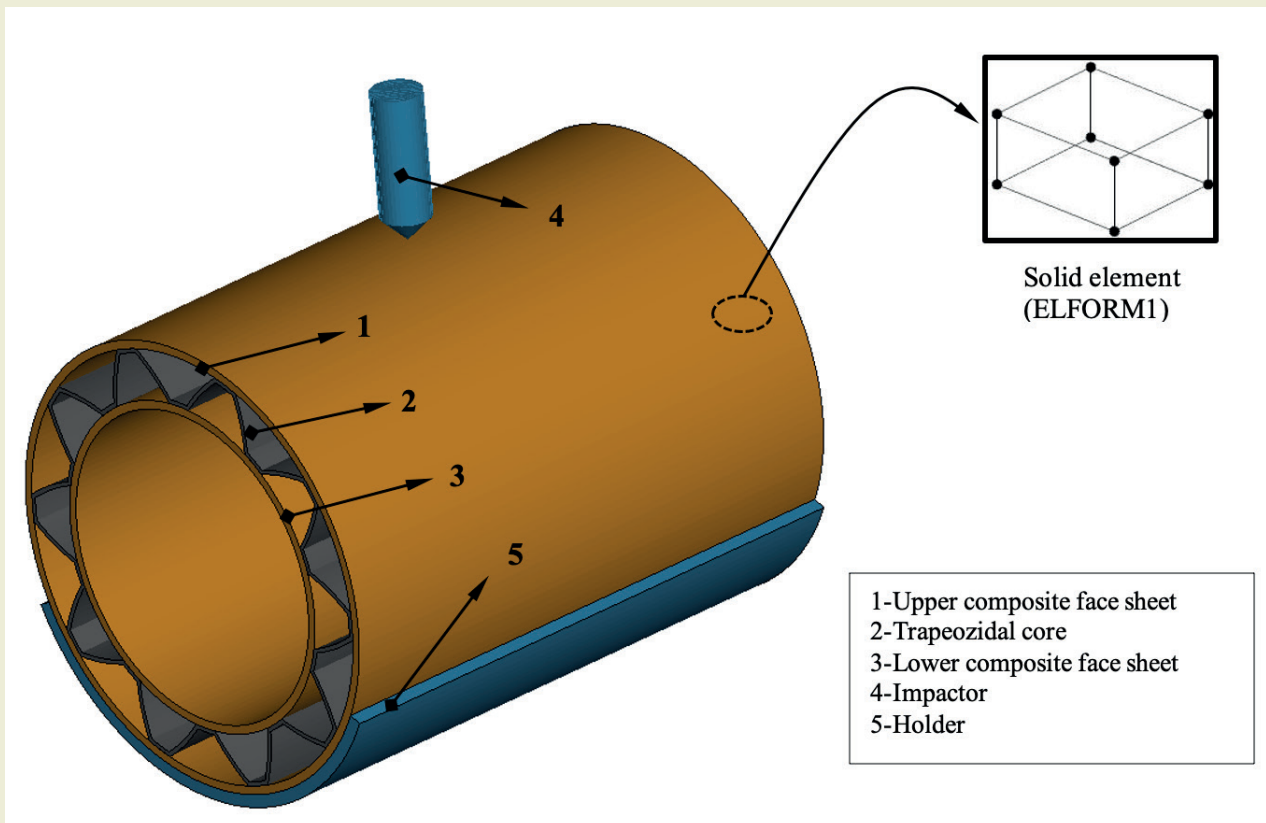
Figure 2. Finite element model of low velocity impact test.

Adhesion here can be achieved in two ways. First, it can be achieved by defining a thin interfacial material between the top cover and the core in the middle. Or it can be achieved by using an adhesion surface that performs the same task. Dogan et al. [19] found this method to be effective instead of using an intermediate material. In this study, The CONTACT_AUTOMATIC SURFACE TO SURFACE TIEBREAK contact board was used to adhere the top and bottom cover to the core material in between. While adhesion is achieved here, separations occur based on the bilinear traction-separation law. With this contact card, the nodes making contact in the beginning connect with each other according to the following criterion.

$$\left(\frac{|\sigma_n|}{NFLS}\right)^2 + \left(\frac{|\sigma_s|}{SFLS}\right)^2 \geq 1 \qquad (1)$$

Here, while σ_n and σ_s are the current normal and shear stresses, NFLS and SFLS are respectively the interface and shear strength. When the condition of Equation (1) is met, interface node stress is decreased to zero and the connection between the nodes is released. The contact parameters for Araldite 2015, which was used as the adhesive material in this research, are provided in ▶Table 1.

2.3. MAT_54-55: Enhanced Composite Damage Model

The mechanical properties of the CFRP material used in the study are given in ▶Table 2-3. The most commonly used model in the analysis of composite structures is the *MAT 54-55* material model. In the material model, it is assumed that the material is orthotropic and linearly elastic in the absence of any damage. In this model, *MAT 54* damage criterion was proposed by Chang and *MAT 55* damage criterion was proposed by *Tsai-Wu*. The working principle of this material model and
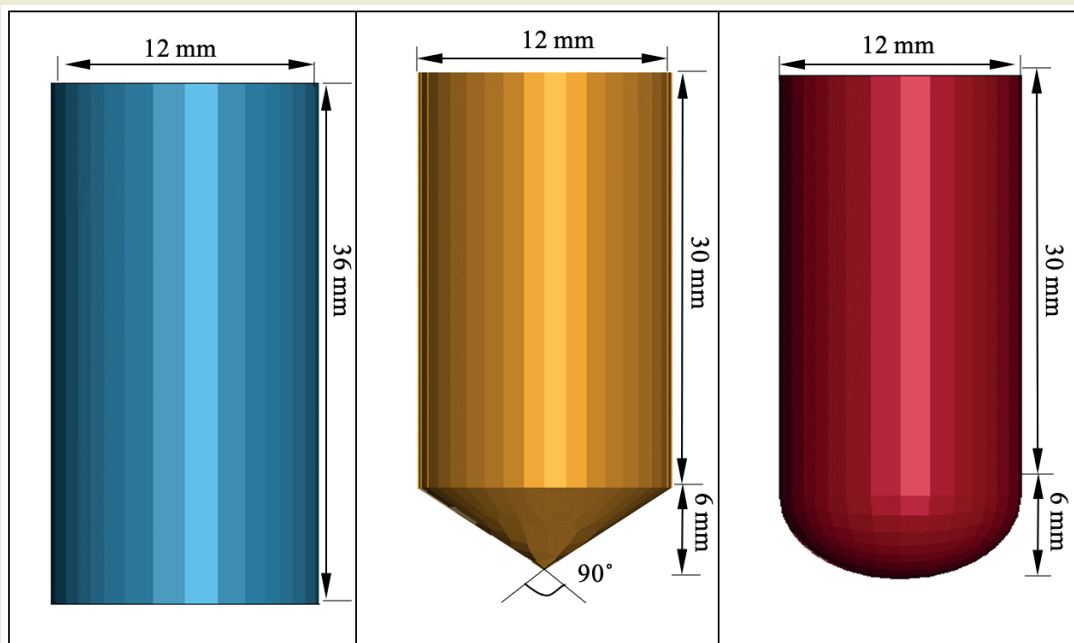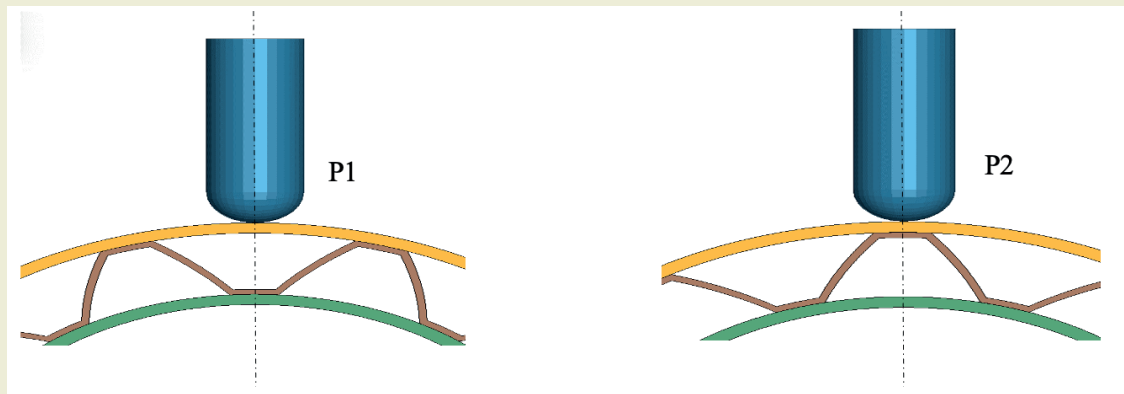

Figure 3. Impactor's dimensions.

Figure 4. Impact points.

Table 1. Cohesive parameters of delamination between core and face sheets interfaces [4].

Contact Tiebreak Variable	Value	Units
NFLS	21.63×10^9	Pa
SFLS	17.9×10^9	Pa
PARAM	1	-
ERATEN	430	N/m
ERATES	4700	N/m
CT2CN	1	-
CN	8080	Pa/m

Table 2. Mechanical parameters of the twill CFRP composite [18].

Symbol	Value	Unit
ρ	1500	kg/m³
E_a, E_b	43.7	GPa
E_c	14.57	GPa
v_{ab}	0.21	-
v_{bc}	0.21	-
v_{ca}	0.21	-
G_{ab}	14.18	GPa
G_{bc}	14.65	GPa
G_{ca}	14.65	GPa
S_{aT}	0.589	GPa
S_{aC}	0.1096	GPa
S_{bT}	0.589	GPa
S_{bC}	0.1096	GPa
S_{ab}	0.1082	GPa

MAT 22 model is the same, but additionally includes compression damage mode. The *Chang–Chang criterion* (*MAT 54*) is given below;

Tensile fibre ($\sigma_{11} > 0$).

$$\left(\frac{\sigma_{11}}{S_1}\right)^2 + \bar{\tau} = 1 \tag{2}$$

All moduli and Poisson's ratios are set to zero when the tensile fibre failure criteria are met, that is $E_1 = E_2 = G_{12} = v_{12} = v_{21} = 0$ All the stresses in the elements are reduced to zero, and the element layer has failed.

Failure mode for compressive fibre ($\sigma_{11} > 0$),

$$\left(\frac{\sigma_{11}}{S_{12}}\right)^2 = 1 \tag{3}$$

Failure mode for tensile matrix ($\sigma_{11} > 0$),

$$\left(\frac{\sigma_{22}}{S_2}\right)^2 + \bar{\tau} = 1 \tag{4}$$

Failure mode for compressive matrix

$$\left(\frac{\sigma_{22}}{2S_{12}}\right)^2 + \left[\left(\frac{C_2}{2S_{12}}\right) - 1\right]\frac{\sigma_{22}}{C_2} + \bar{\tau} = 1 \tag{5}$$

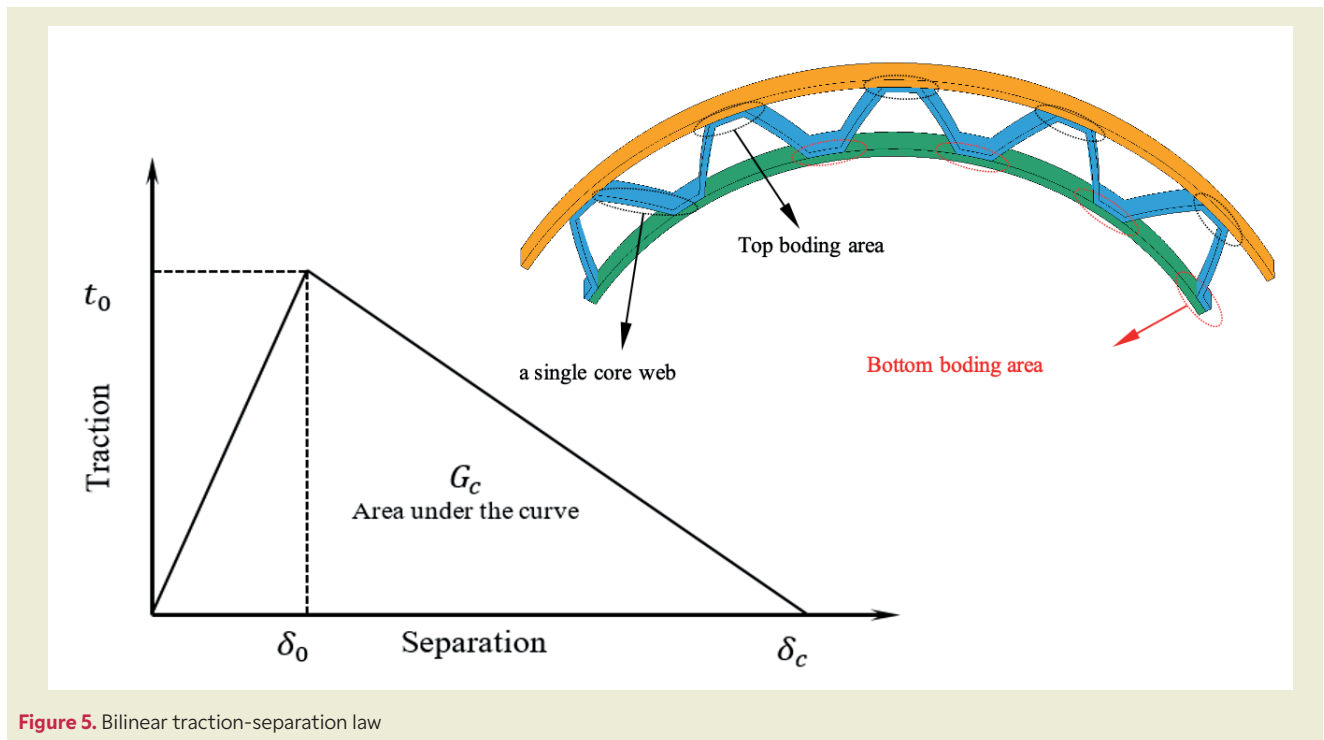Where E_1 and E_2 are the longitudinal and transverse

Figure 5. Bilinear traction-separation law

elastic moduli, respectively, G_{12} is the shear modulus, υ_{12} and υ_{21} are the in-plane Poisson's ratios.

Table 3. Failure parameters of the CFRP composite.

Symbol	Unit
DFAILM	0.0
DFAILS	0.0
DFAILT	0.0
DFAILC	0.0
TFAIL	0.16
Alpha	0.0
Soft	0.7
FBRT	1
YCFAC	3
EFS	0.90

3. Results and Discussion

Low-velocity impact tests are usually applied to determine the behavior of the material under impact load. These tests provide information about the mechanical performance of the material. The most important graphs obtained as a result of impact tests are given in ▶**Figure 6**. These results contain important information for researchers about material mechanics. For example, in the Contact force-time graph in ▶**Figure 6a**, after the impactor contacted the specimen, the force increased to the maximum point (peak force, PF) and then returned. Fluctuations occurred at the peak point, where changes in the force value occurred due to damage to the layers at the point of contact. We can see this reversal in ▶**Figure 6b** from the displacement movements of the impactor. ▶**Figure 6c** shows the absorbed energy (AE) value of the difference between the initial energy of the impactor and the probe energy. The impactor bounced back from the specimen surface. Because it continues, its energy at a certain speed after the contact is broken. With these graphs, appropriate material and structure selection can be made by evaluating the mechanical conditions experienced in the impact scenario.

Contact force-time, absorbed energy-time, contact force-displacement and velocity-time graphs for different impactors of circular sandwich structure with Trapeozidal core are given in ▶**Figure 7**. The impact test here was applied at point P1. In the contact force-time graph in ▶**Figure 7a**, the force reaches a maximum point due to the impactor contacting the specimen surface and then returns back to zero point with the energy discharge. The same scenario was observed for all three impactors. With 5 J impact energy, impact simulation
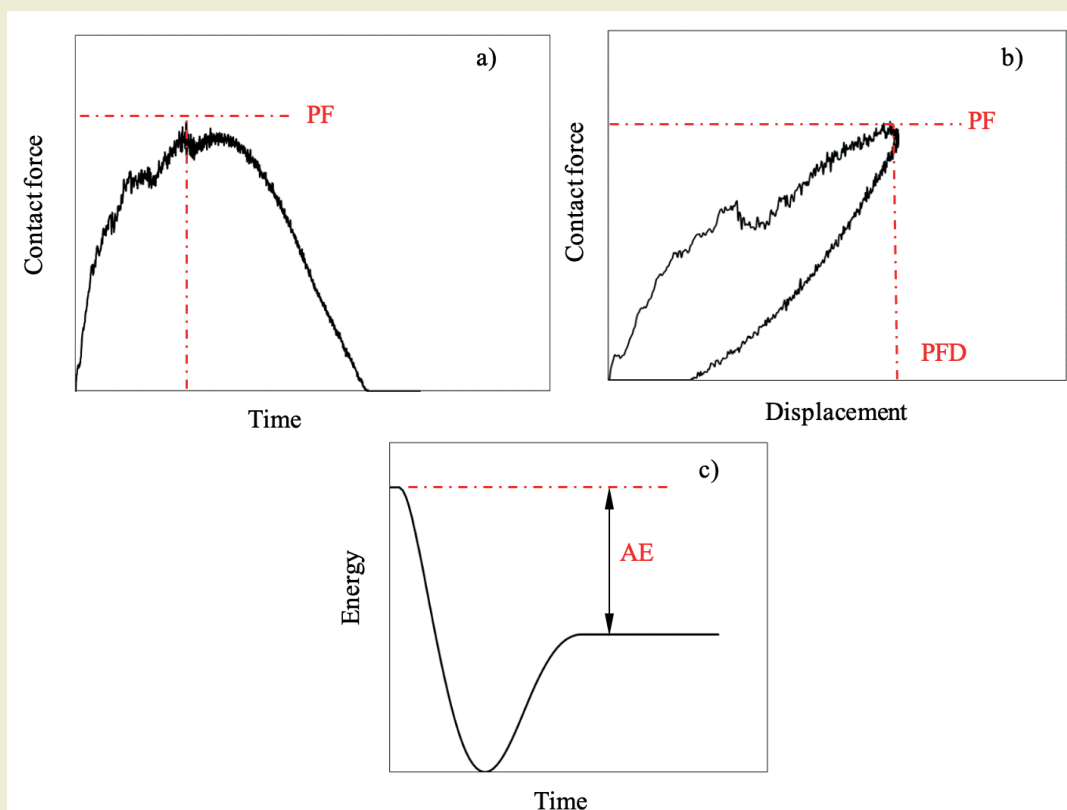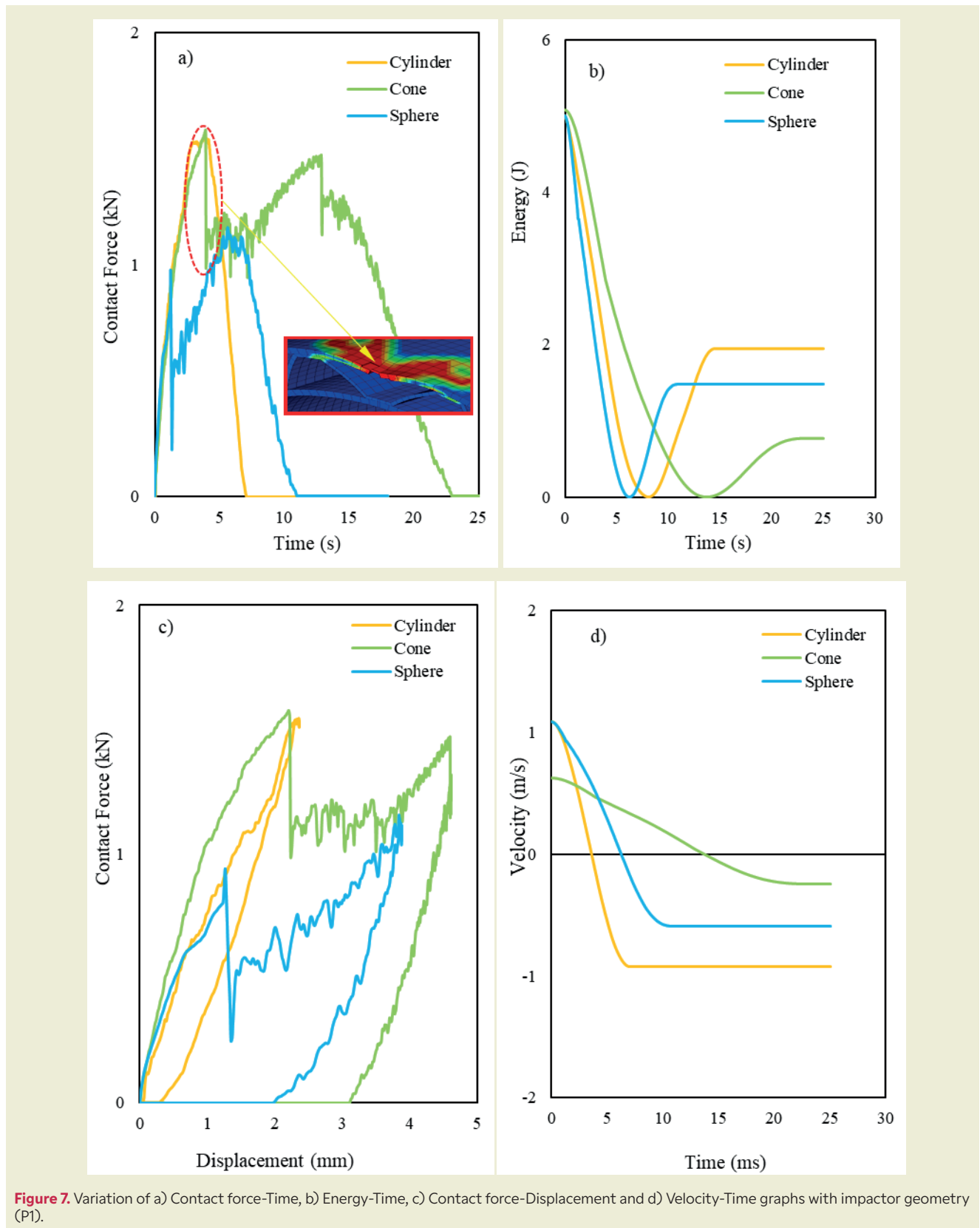

Figure 6. Composite cylinder structures under impact load a) Contact force-time, b) Contact force -displacement and c) Energy-time graphs.

was performed with cylindrical, conical and spherical impactors. The peak contact forces for cylindrical, conical and spherical impactors are 1.55, 1.58 and 1.16 kN respectively. Accordingly, the highest peak force value among these three impactors was obtained in

the sphere impactor [13]. When the graph is examined in detail, it is determined that the force increases and decreases linearly to the peak point in the impact with the cylinder. However, in the cone and sphere impactor, the force increased up to a point and then dropped

Figure 7. Variation of a) Contact force-Time, b) Energy-Time, c) Contact force-Displacement and d) Velocity-Time graphs with impactor geometry (P1).

sharply. It is understood that damage to the top layer occurred here. Therefore, the point of contact of the impactor at the moment when this force fell is shown on the graph. In ▶Figure 7b, the initial energy is 5 J for all three impactors in the energy-time graph. But at the end of the impact, the remaining energies for the cylinder, cone and sphere impactor are 3.16 J, 0.77 J and

1.48 J respectively. To calculate the energy absorption efficiency, we divide this energy difference (final energy - initial energy) by the initial energy. Therefore, the energy absorption efficiency (η) for cylinder, cone and sphere impactor is 0.28, 0.92 and 0.70 respectively. The highest energy absorption was obtained in the impact simulation with the cone impactor. When the displace-
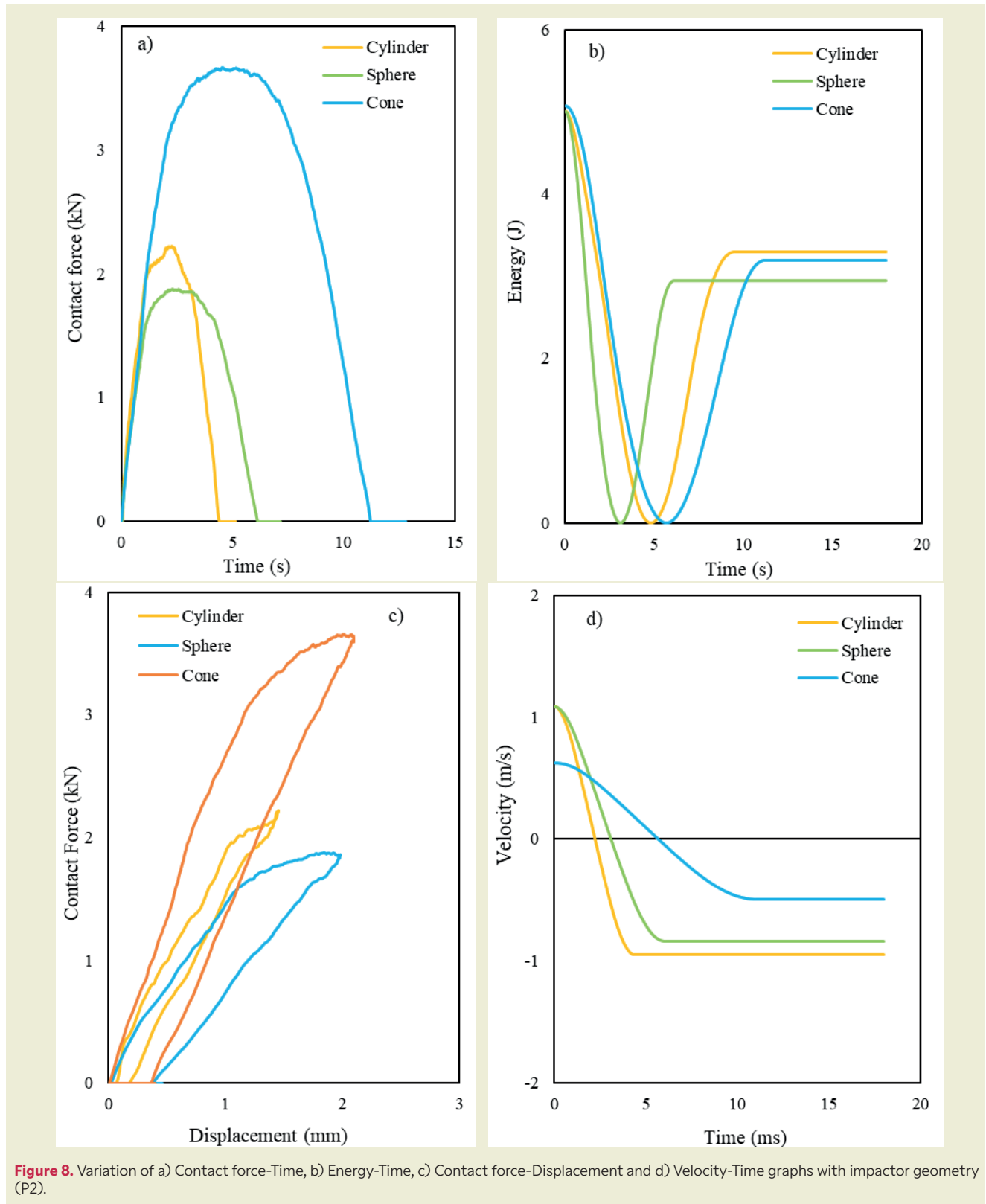
Figure 8. Variation of a) Contact force-Time, b) Energy-Time, c) Contact force-Displacement and d) Velocity-Time graphs with impactor geometry (P2).
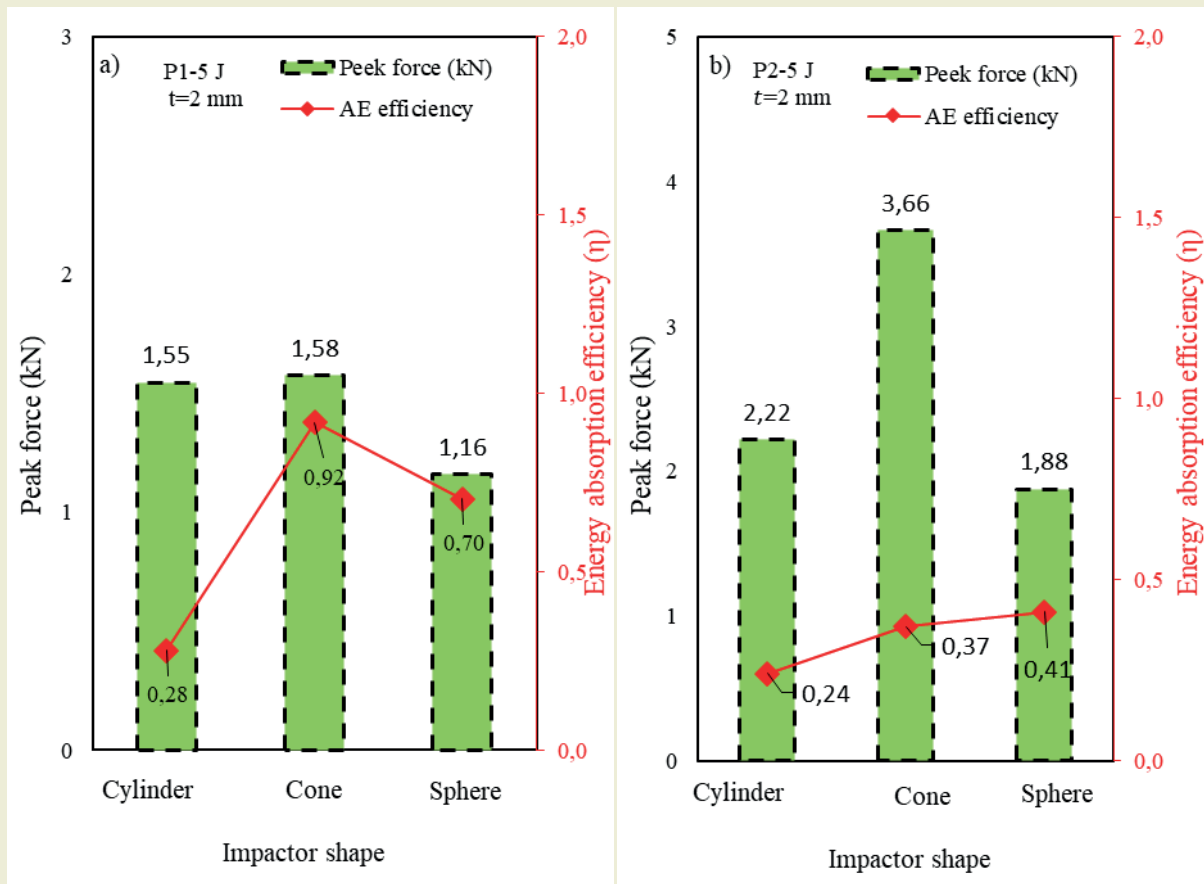
Figure 9. Variation of Contact force, Absorbed energy efficiency values for a) P1, b) P2 impact points (Facesheets thickness *t*= 2 mm).
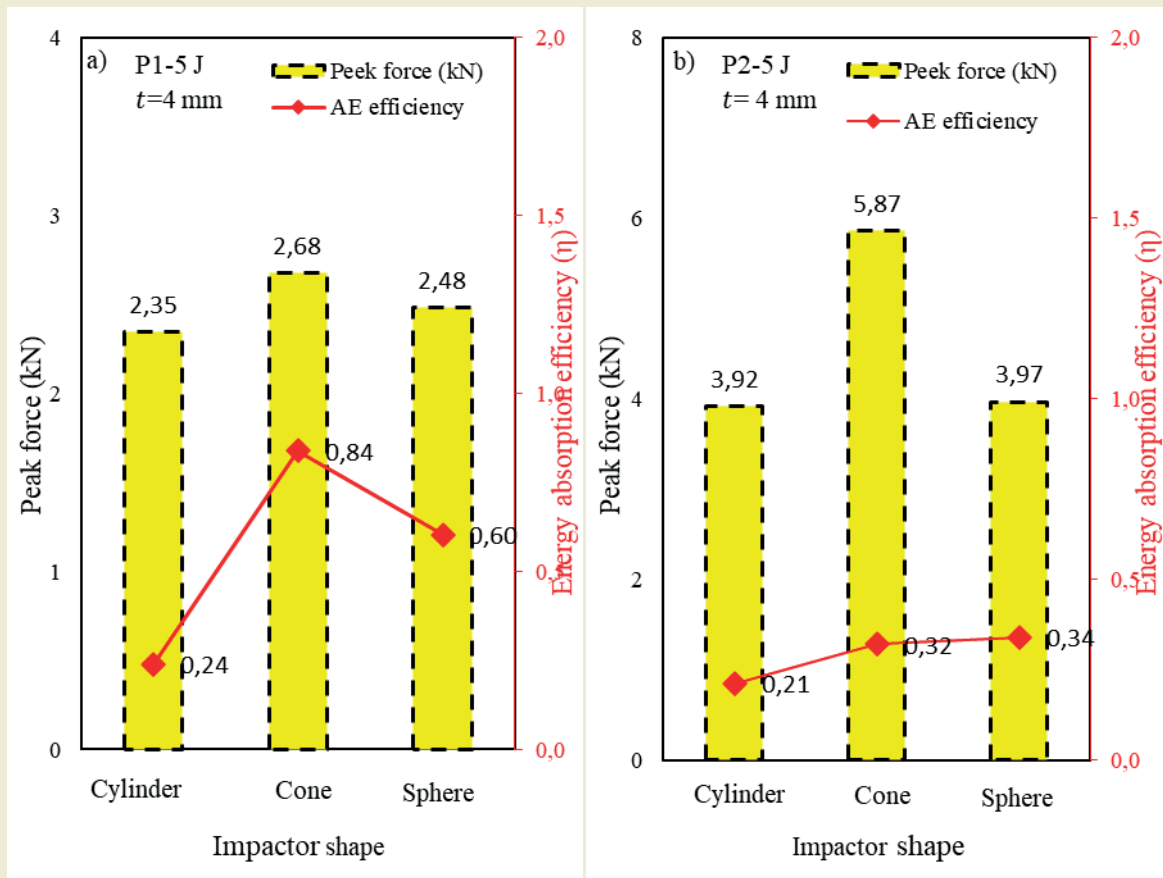
Figure 10. Variation of Contact force, Absorbed energy efficiency values for a) P1, b) P2 impact points (Facesheets thickness *t*= 4 mm).

ments are analyzed in the contact force-displacement graph in ▶**Figure 7c**, 2.82, 4.62 and 3.88 mm displacement occurred for the cylinder, cone and sphere impactor, respectively. ▶**Figure 7d** shows the changes in the velocity-time graph. When the graph is analyzed, it is seen that the velocity decreases to 0 and then moves in the negative direction. This indicates that the velocity decreases to zero after the impactor makes contact and then moves in the opposite direction. In ▶**Figure 8**, similar graphs are given for point P2. In ▶**Figure 8a**, in the contact force-time graph, the force goes up and down to the peak point without oscillation. Therefore, it is understood that a large deformation does not occur here, i.e. at point P2, like point P1. This is because this point is supported by the core structure [16]. In the energy-time graph in ▶**Figure 8b**, it is seen that the final output energy values are close to the initial energy values. Therefore, it is determined that there is less energy absorbed from P1. In the contact force-displacement graph in ▶**Figure 8c**, it is more clearly seen that the force goes to the peak point and returns back again. In ▶**Figure 8d**, the changes in the velocity-time graph are similar.

▶**Figure 9** shows the peak force and energy absorption efficiency values of the Trapeozidal sandwich structure under different impactors. In ▶**Figure 9a**, the peak force value for impact point P1 is the highest with 1.58 kN with cone impactor. Energy absorption efficiency value was also obtained with cone impactor. In ▶**Figure 9b**, for impact point P2, the cone impactor has the highest contact force value with 3.66 kN. The energy absorption efficiency of 0.41, i.e. 40%, was obtained with the sphere impactor. ▶**Figure 10** shows the peak force and energy absorption efficiency values under different impactors for facesheet thickness t=4 mm. It was observed that the maximum contact force increased for all three specimens when the facesheets thickness t was increased from 2 mm to 4 mm [21]. On the other hand, the energy absorbed value also decreased. The peak contact force value and the highest energy absorption efficiency value were obtained with cone impactor.

In ▶**Table 4** and ▶**Table 5**, Tensile fiber mode, Compressive fiber mode, Tensile matrix mode and Compressive matrix mode damages are shown separately for different impact points (P1 and P2). The damages in the core structure for 5 J impact for different impactors are compared. Here, the regions shown in red color represent the damaged areas and the regions shown in blue represent the areas where no damage occurred [22]. First of all, it is seen that the deformation at point P1 is large because it is not supported by the core [13]. However, it was determined that the effect of the damage spread over a wider area. It was mentioned in the previous section that this effect causes large fluctuations in the graphic structures. At P2, the damage was more stable and localized compared to P1 since it was supported by the core structure [18]. It is seen that the Cone impactor has a more destructive effect. It is understood that the core structure is a very important parameter against impact [4], [23], [24]. However, it is seen that matrix damage is the most dominant damage type.

One of the most important conveniences offered by the finite element method is to see the deformations at the desired point during the impact simulation [25]. ▶**Figure 11** shows the Contact force-time result obtained as a result of the impact at point P1 for the cone impactor. When the graph is examined, the force value increased to the peak point with the contact of the impactor to the specimen. Then a sharp decrease in the force value occurred here. While the force continued to fluctuate, the second sharp drop occurred. In the last part, it is seen that the force value reaches zero point by making certain oscillations and fluctuations. In general, when the graph is analyzed, a more fluctuating and oscillating contact force value is obtained than other graphs due to the destructive effect of the cone tip [2], [26]. Each movement mentioned here provides valuable information about material mechanics to researchers and engineers working in this field. Therefore, each point should be analyzed very carefully [27]. Shortly after the impactor contacts the cylindrical sandwich specimen, the damage starts (Phase 1). As the force increased, the stresses on the elements here increased. Then the damage occurred with element deletion (Phase 2). As the force increased, the damage area, i.e. the area of the red zone, increased (Phase 3). Since the elements were deleted due to the force and therefore stresses, there was a sharp decrease in the contact force value (Phase 4). The final state of the damage in the contact area as the impactor breaks contact is given below (Phase 5-6).

4. Conclusions

In this study, the impact performance of cylindrical sandwich structure with Trapeozidal core under different geometries of impactors was investigated by the finite element method. The effects of impactor shape, facesheets thickness and the impact point on Peak contact force, absorbed energy efficiency, maximum displacement and damage deformation were investigated. Low velocity impact simulations were performed in *LS DYNA* finite element program. The results obtained at the end of the study can be listed as follows;

- In general, the contact force values at P2 are higher than P1. Core support has a significant effect on the contact force.

- Peak force variation values for cylinder, cone and sphere tipped impactors at P1 and P2 points were 43.5%, 132.3% and 62.2%, respectively. The biggest change at P1 and P2 points occurred in the cone impactor.

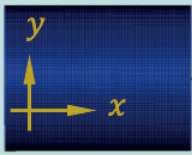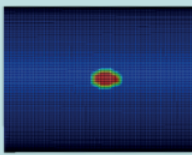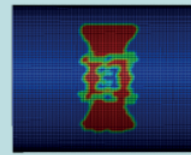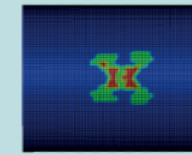**Table 4.** Deformation images under different impactor force (P1).

Table 5. Deformation images under different impactor force (P2).
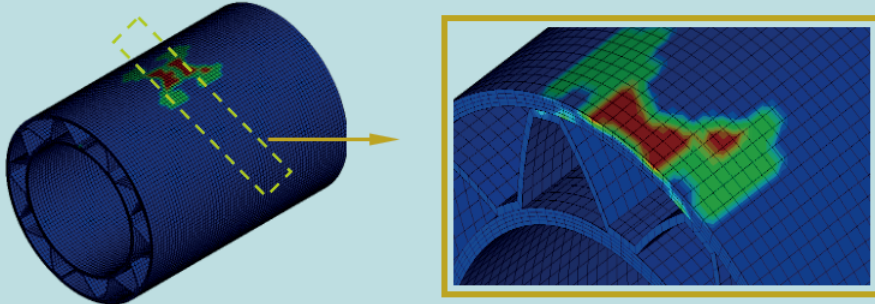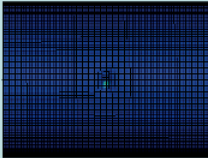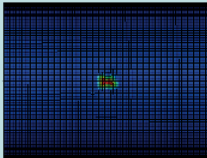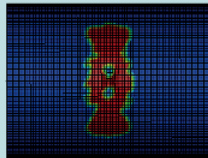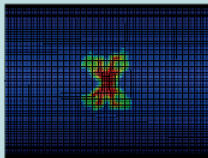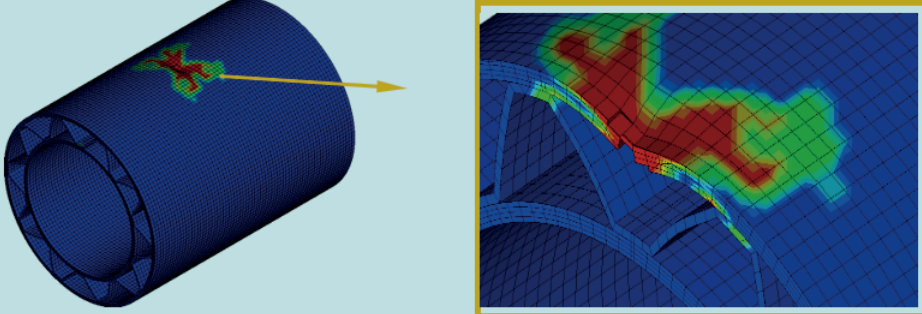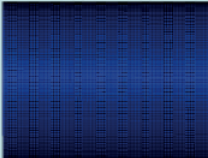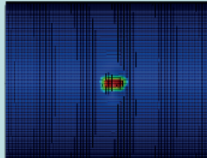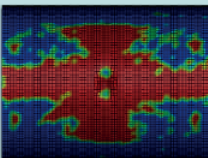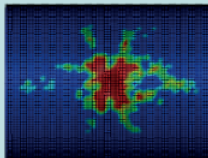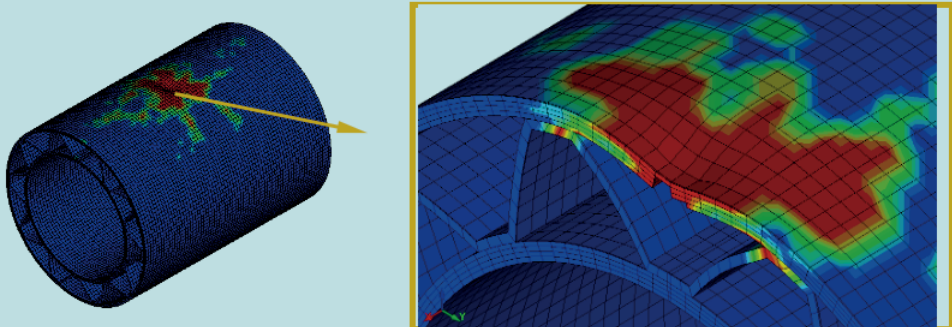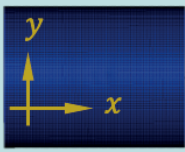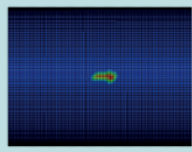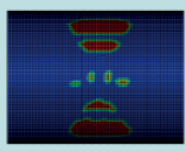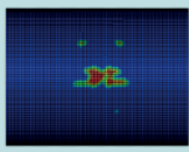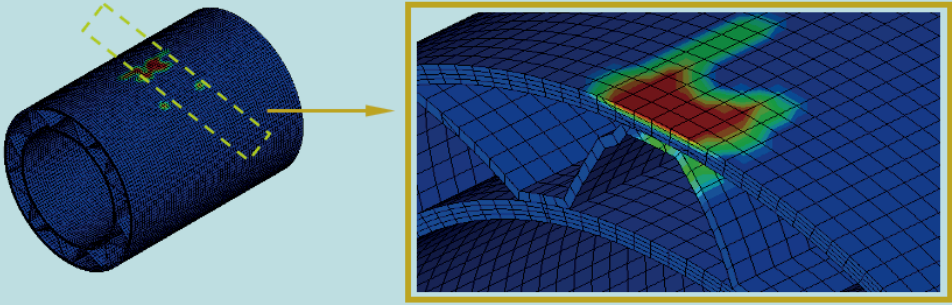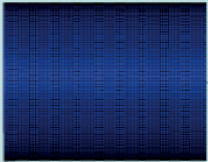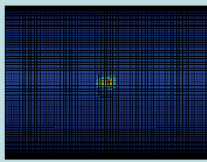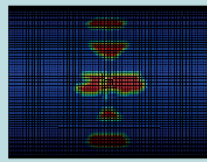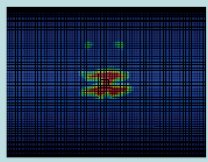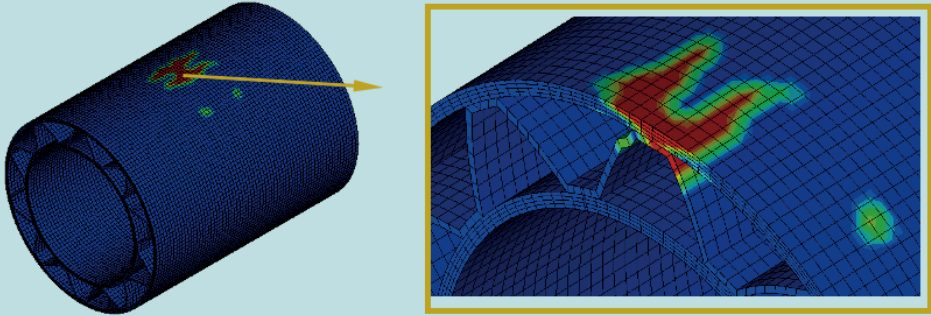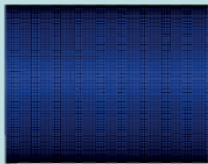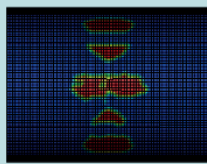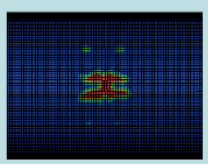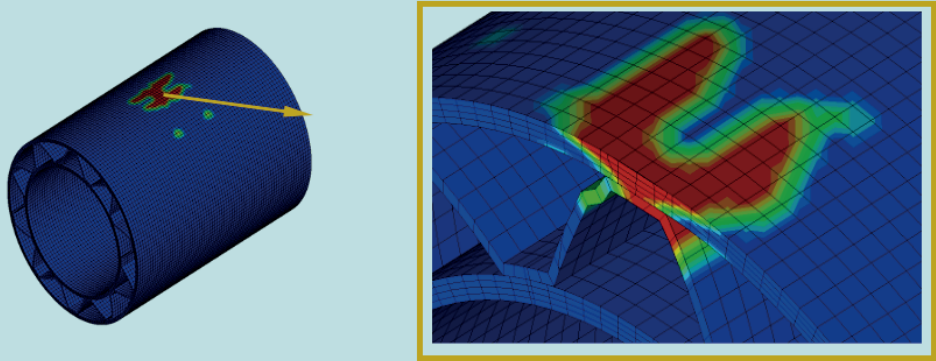
E (J)		Tensile fiber mode	Compressive fiber mode	Tensile matrix mode	Compressive matrix mode
Cylinder, 5 J	Top face				
	Section view				
Cone 5 J	Top face				
	Isometric				
Sphere 5 J	Top face				
	Isometric				

Figure 11. Matrix damage progress for cone impactor (P1).

- The peak force value and energy absorption efficiency value obtained with the Cone impactor are higher than the others. This is due to the fact that the contact area of the impactor with the specimen is small and destructive.
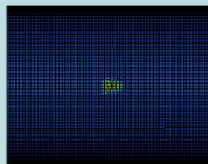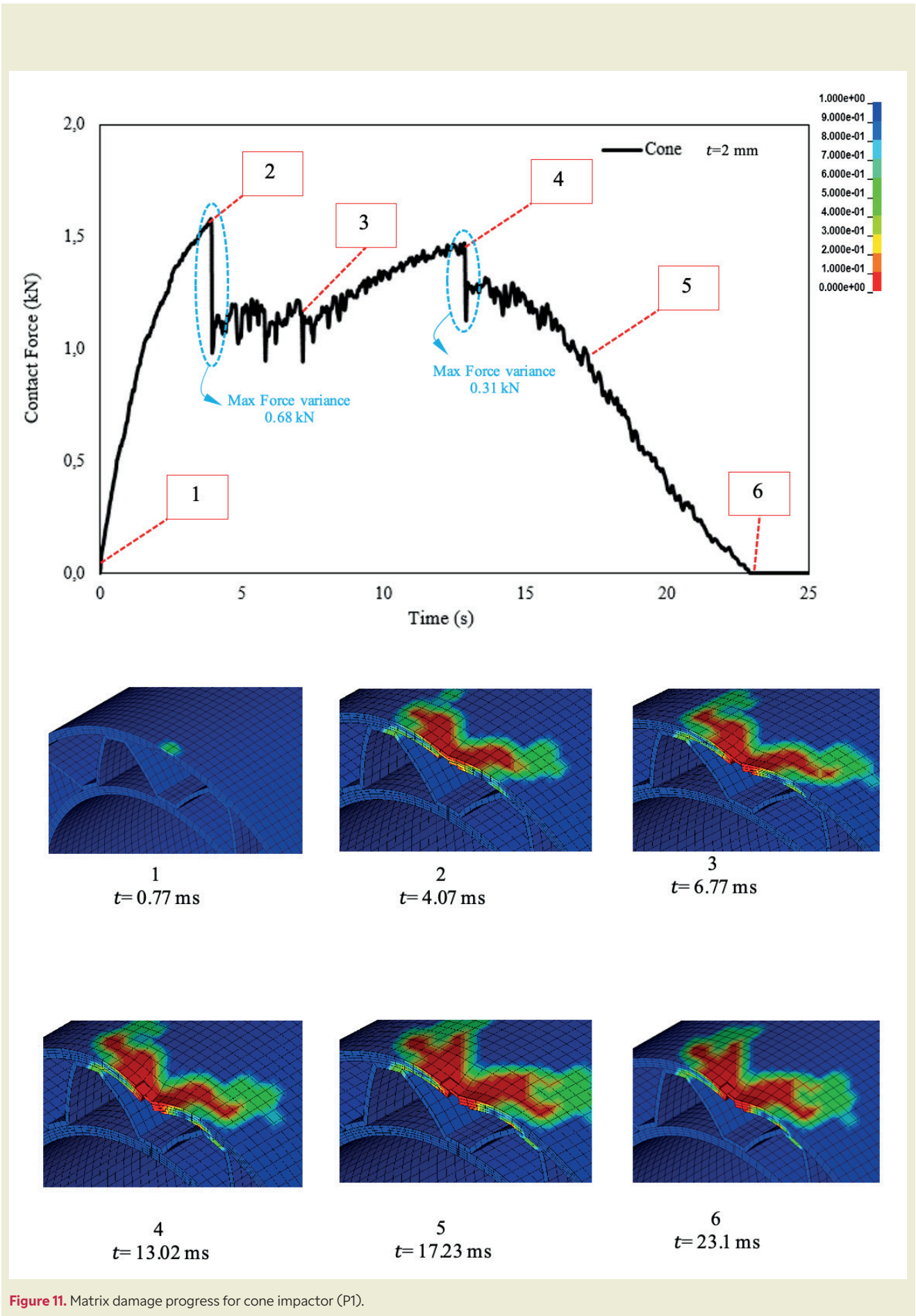
- The largest displacement as a result of the impact occurred with the cone impactor.

- The impactor geometry was found to have a significant effect on the energy absorption efficiency.

- For all three impactors, the largest and dominant damage type was matrix damage.

- This study has the potential to contribute to the literature if it is supported by an experimental study in future research.

Research ethics

Not applicable.

Author contributions

The author has accepted responsibility for the entire content of this manuscript and approved its submission.

Competing interests

The author states no conflict of interest.

Research funding

None declared.

Data availability

Not applicable.

Peer-review

Externally peer-reviewed.

References

[1] Crupi, V., Kara, E., Epasto, G., Guglielmino, E., & Aykul, H. (2015). Prediction model for the impact response of glass fibre reinforced aluminium foam sandwiches. *International Journal of Impact Engineering, 77*, 97–107. https://doi.org/10.1016/j.ijimpeng.2014.11.012

[2] Kazemianfar, B., Esmaeeli, M., & Nami, M. R. (2020). Response of 3D woven composites under low velocity impact with different impactor geometries. *Aerospace Science and Technology, 102.* https://doi.org/10.1016/j.ast.2020.105849

[3] Solmaz, M. Y., & Topkaya, T. (2020). The flexural fatigue behavior of honeycomb sandwich composites following low velocity impacts. *Applied Sciences (Switzerland), 10*(20), 1–14. https://doi.org/10.3390/app10207262

[4] Bozkurt, I., Kaman, M. O., & Albayrak, M. (2024). Experimental and numerical impact behavior of fully carbon fiber sandwiches for different core types. *Journal of the Brazilian Society of Mechanical Sciences and Engineering, 46*(5), 318. https://doi.org/10.1007/s40430-024-04865-3

[5] He, W., Lu, S., Yi, K., Wang, S., Sun, G., & Hu, Z. (2019). Residual flexural properties of CFRP sandwich structures with aluminum honeycomb cores after low-velocity impact. *International Journal of Mechanical Sciences, 161–162*, 105026. https://doi.org/10.1016/j.ijmecsci.2019.105026

[6] He, W., Liu, J., Tao, B., Xie, D., Liu, J., & Zhang, M. (2016). Experimental and numerical research on the low velocity impact behavior of hybrid corrugated core sandwich structures. *Composite Structures, 158*, 30–43. https://doi.org/10.1016/j.compstruct.2016.09.009

[7] Chen, Y., Fu, K., Hou, S., Han, X., & Ye, L. (2018). Multi-objective optimization for designing a composite sandwich structure under normal and 45° impact loadings. *Composites Part B: Engineering, 142*, 159–170. https://doi.org/10.1016/j.compositesb.2018.01.020

[8] Zhang, X., Xu, F., Zang, Y., & Feng, W. (2020). Experimental and numerical investigation on damage behavior of honeycomb sandwich panel subjected to low-velocity impact. *Composite Structures, 236*, 111882. https://doi.org/10.1016/j.compstruct.2020.111882

[9] He, W., Liu, J., Wang, S., & Xie, D. (2018). Low-velocity impact behavior of X-Frame core sandwich structures – Experimental and numerical investigation. *Thin-Walled Structures, 131*, 718–735. https://doi.org/10.1016/j.tws.2018.07.042

[10] Demircioğlu, T. K., Balıkoğlu, F., İnal, O., Arslan, N., & Ataş, A. (2018). Experimental investigation on low-velocity impact response of wood skinned sandwich composites with different core configurations. *Materials Today Communications, 17*, 31–39. https://doi.org/10.1016/j.mtcomm.2018.08.003

[11] Wang, J., Waas, A. M., & Wang, H. (2013). Experimental and numerical study on the low-velocity impact behavior of foam-core sandwich panels. *Composite Structures, 96*, 298–311. https://doi.org/10.1016/j.compstruct.2012.09.002

[12] Rong, Y., Liu, J., Luo, W., & He, W. (2018). Effects of geometric configurations of corrugated cores on the local impact and planar compression of sandwich panels. *Composites Part B: Engineering, 152*, 324–335. https://doi.org/10.1016/j.compositesb.2018.08.130

[13] Liu, J., He, W., Xie, D., & Tao, B. (2017). The effect of impactor shape on the low-velocity impact behavior of hybrid corrugated core sandwich structures. *Composites Part B: Engineering, 111*, 315–331. https://doi.org/10.1016/j.compositesb.2016.11.060

[14] Khalkhali, A., Geran Malek, N., & Bozorgi Nejad, M. (2020). Effects of the impactor geometrical shape on the non-linear low-velocity impact response of sandwich plate with CNTRC face sheets. *Journal of Sandwich Structures and Materials, 22*(4), 962–990. https://doi.org/10.1177/1099636218778998

[15] Shirbhate, P. A., & Goel, M. D. (2023). Investigation of effect of perforations in honeycomb sandwich structure for enhanced blast load mitigation. *Mechanics of Advanced Materials and Structures, 30*(17), 3463–3478. https://doi.org/10.1080/15376494.2022.2076958

[16] Yalkın, H. E., Karakuzu, R., & Alpyıldız, T. (2023). Low-velocity impact behaviors of sandwich composites with different structural configurations of foam core: Numerical study and experimental validation. *Physica Scripta, 98*(11). https://doi.org/10.1088/1402-4896/ad008f

[17] Nouri Damghani, M., & Mohammadzadeh Gonabadi, A. (2019). Numerical study of energy absorption in aluminum foam sandwich panel structures using drop hammer test. *Journal of Sandwich Structures and Materials, 21*(1), 3–18. https://doi.org/10.1177/1099636216685315

[18] Bozkurt, I., Kaman, M. O., & Albayrak, M. (2023). Low-velocity impact behaviours of sandwiches manufactured from fully carbon fiber

composite for different cell types and compression behaviours for different core types. *Materialprüfung/Materials Testing, 65*(9), 1349–1372. https://doi.org/10.1515/mt-2023-0024

[19] Dogan, F., Hadavinia, H., Donchev, T., & Bhonge, P. S. (2012). Delamination of impacted composite structures by cohesive zone interface elements and tiebreak contact. *Central European Journal of Engineering, 2*(4), 612–626. https://doi.org/10.2478/S13531-012-0018-0

[20] Albayrak, M., & Kaman, M. O. (2021). Production of curved surface composites reinforced with rubber layer. *European Journal of Technic, 11*(1), 19–22. https://doi.org/10.36222/ejt.824761

[21] Atas, C., Icten, B. M., & Küçük, M. (2013). Thickness effect on repeated impact response of woven fabric composite plates. *Composites Part B: Engineering, 49*, 80–85. https://doi.org/10.1016/j.compositesb.2013.01.019

[22] Bozkurt, I., & Kaman, M. O. (2022). LS-DYNA MAT162 finding material inputs and investigation of impact damage in carbon composite plates. In *XVI International Research Conference 2022*.

[23] Zhao, T., et al. (2020). An experimental investigation on low-velocity impact response of a novel corrugated sandwiched composite structure. *Composite Structures, 252*, 112676. https://doi.org/10.1016/j.compstruct.2020.112676

[24] Kaman, M. O., Solmaz, M. Y., & Turan, K. (2010). Experimental and numerical analysis of critical buckling load of honeycomb sandwich panels. *Journal of Composite Materials, 44*(24), 2819–2831. https://doi.org/10.1177/0021998310371541

[25] Gama, B. A., Bogetti, T. A., & Gillespie, J. W. Jr. (2009). Progressive damage modeling of plain-weave composites using LS-DYNA composite damage model MAT162. In *7th European LS-DYNA Conference*.

[26] Icten, B. M., Kiral, B. G., & Deniz, M. E. (2013). Impactor diameter effect on low velocity impact response of woven glass epoxy composite plates. *Composites Part B: Engineering, 50*, 325–332. https://doi.org/10.1016/j.compositesb.2013.02.024

[27] Albayrak, M., Kaman, M. O., & Bozkurt, I. (2023). The effect of lamina configuration on low-velocity impact behaviour for glass fiber/rubber curved composites. *Journal of Composite Materials, 57*(11), 1875–1908. https://doi.org/10.1177/00219983231164950